Spontaneous Roughening: Fundamental Limits in Si(100) Halogen Etch Processing

Cari F. Herrmann, Dongxue Chen, and John J. Boland*

Venable and Kenan Laboratories, Department of Chemistry, University of North Carolina at Chapel Hill, Chapel Hill, North Carolina 27599-3290

(Received 4 March 2002; published 8 August 2002)

A dynamical scanning tunneling microscopy and density functional theory study of the thermodynamic stability of halogen-terminated Si(100) surfaces is presented. Significant steric repulsions are shown to exist on all halogen-terminated Si(100) surfaces. These repulsions are the driving force for a roughening phenomenon, which is favored for all halogens except fluorine. Since roughening is an intrinsic property of these surfaces, it sets a lower bound on the atomic scale perfection that can be achieved using halogen etch processing.

DOI: 10.1103/PhysRevLett.89.096102 PACS numbers: 81.65.Rv, 68.37.Ef, 71.15.Mb

Future developments in information and communication technologies hinge on the ability to process Si(100) substrates with ever increasing precision. As dimensions are reduced, device performance becomes critically sensitive to uncontrolled variations in channel length and interface roughness. Device features are typically defined using lithography and physicochemical processing, the latter involving the use of halogen gas-phase etchants. It is widely assumed that there are no etch-related obstacles preventing continued refinement and device miniaturization. In chemical etching, the final surface morphology is controlled by the stability of exposed (100) surfaces and the relative etch rates at terrace, step, and kink sites on this surface [1]. To date it has been assumed that kinetic effects dominate so that by enhancing the relative etch rates at kink and step sites over terrace sites it is possible, at least in principle, to etch atomically smooth surfaces.

Here we present a study of the intrinsic thermodynamic stability of halogen-terminated Si(100) surfaces. Using dynamical scanning tunneling microscopy (STM) and density functional theory (DFT) calculations, we show that defect-free halogen-covered Si(100) surfaces are intrinsically unstable and susceptible to spontaneous roughening. This instability is the result of steric effects and is observed for all halogens except fluorine (which is already known to yield rough surfaces). These results indicate that an atomically smooth Si(100) morphology cannot be easily realized using present day halogen etch processing.

The samples used in this study were prepared by annealing 0.3–1.0 Ω cm phosphorous-doped Si(100) substrates to 1400 K to remove the native oxide. The clean surface was then heated and exposed to doses up to 3.6×10^4 μA s of Br_2 or Cl_2 (approximately 720 langmuir) using an electrochemical cell [2]. After preparation, the surface was cooled to room temperature and then subsequently heated (300–1000 K) in the STM stage while images (empty state, typically -1.7 V tip bias) were recorded. At each temperature, images were acquired for several hours, so that recorded events either were repetitive (e.g., site hopping) or occurred on time scales that were slow compared to our imaging speed (typically 100 nm/sec).

To determine the intrinsic stability of halogen-terminated Si(100) surfaces, we studied the surface morphology under a variety of exposure conditions. Prolonged halogen exposure at low temperature produced poorly ordered surfaces. At higher temperatures the order improved, but it was not possible to achieve an atomically smooth surface termination such as that routinely obtained following H exposure [3]. Instead, the resulting surfaces (Fig. 1(a), exposure to Cl_2 at 750 K, quenched and imaged) are invariably rough and composed of dimer vacancy (DV) strings and islands, a morphology that we shall refer to as primary roughening. Real-time dynamical STM studies provide additional insight into the origin of primary roughening. Figures 1(b) and 1(c) (consecutive images recorded on an 800-K Br surface) show the transformation of a 3-DV string into a 5-DV string (white arrows) with the concomitant elongation of a nearby island by two dimer units (black arrows). Since the DV string and island are extended by the same amount, the number of surface Si and Br atoms is conserved, consistent with a roughening process. Similar observations were recorded on the Cl surface [4]. A secondary roughening process is also observed [5]. Figures 1(d) and 1(e) (consecutive images recorded on an 800-K Br surface) show that DV strings can further roughen by rearranging into two single-atom vacancy (SV) strings separated by one or more dimer rows [6].

A more detailed STM analysis actually reveals that the silicon-halogen surface bonds relax into the vacancies created on the roughened surface. Figure 2 shows an image (recorded on an 800-K Br surface) together with a cross section that traverses an area of primary and secondary roughening. Dimers (orange arrows) located between the SV and DV strings appear substantially (~ 0.02 nm) lower than dimers in the surrounding terrace. In addition, terrace dimers (yellow arrows) that border the roughened area also relax, but relaxation is possible for only half of each dimer unit, i.e., only the silicon-halogen bonds that are directly adjacent to the vacancy. Evidently, terrace crowding is severe [7] such that silicon-halogen bonds next to vacancies and on islands of the roughened surface are driven to relax by tilting towards the surface plane.

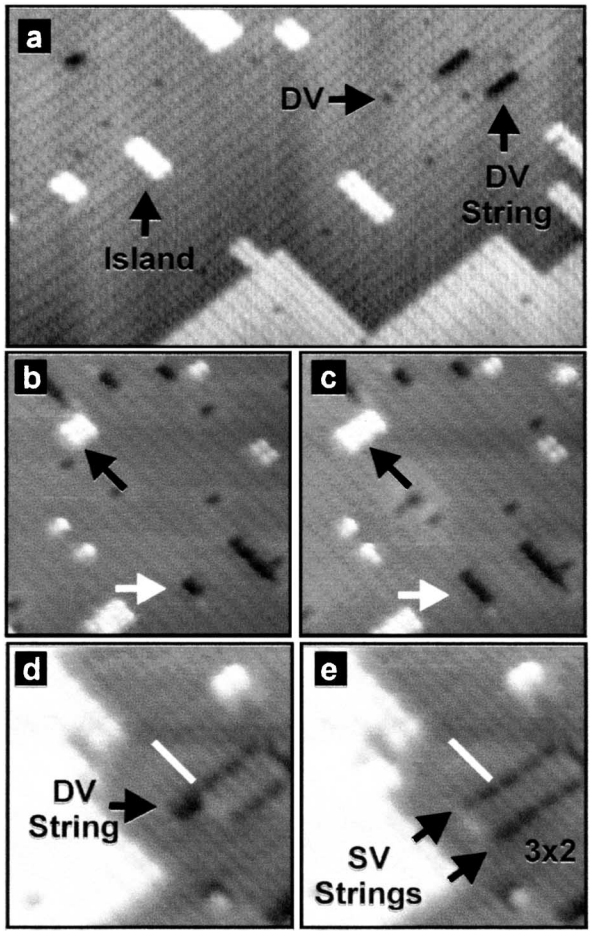

FIG. 1. STM images of halogen-terminated Si(100) surfaces. (a) An image illustrating primary roughening on a Cl surface recorded at 300 K following a saturation exposure at 750 K. (b) and (c) Consecutive real-time images of a primary roughening event on a Br surface recorded at 800 K. (d) and (e) A secondary roughening event on the same Br surface. The white lines in (d) and (e) indicate the same position in the two images.

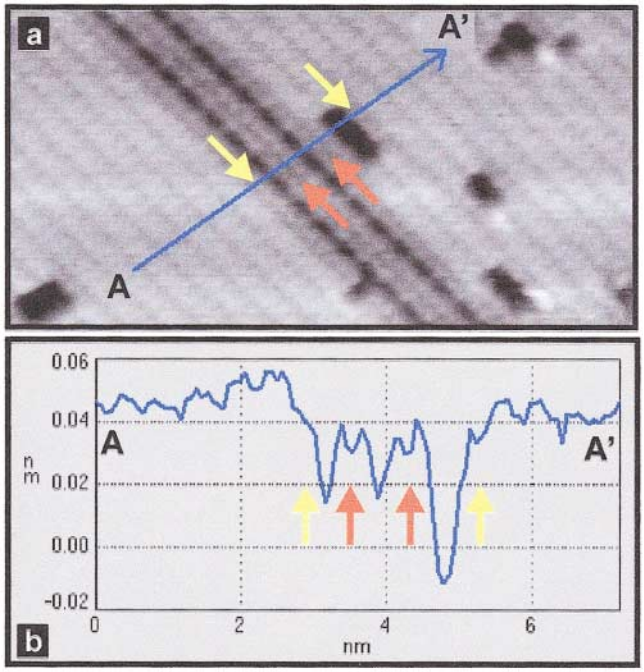

FIG. 2 (color). Evidence for steric interactions on Br-Si(100). (a) STM image recorded at 800 K that illustrates both primary and secondary roughening. The line AA' corresponds to the cross section in (b). The orange arrows indicate the relaxed position of dimers between SV and DV strings. The yellow arrows indicate the relaxed half-dimers that border the roughened areas. The slope in the cross section is due to background subtraction.

DFT calculations were performed to elucidate the driving force for Si(100) roughening. We separate the surface energy into two parts. The first involves the surface energy increase due to roughening itself, and for single layer roughening (see Fig. 1) this is determined by the energies of Si(100) surface steps. The second part is due to the change in adsorption energy associated with the decoration of the roughened surface with halogen atoms. Since smooth and roughened Si(100) surfaces have the same rebonded structure with the same number of surface silicon and halogen atoms, the change in adsorption energy results from differences in the local steric environment of the halogens on these two surfaces. Roughening is energetically favored whenever the surface energy increase is offset by a reduction in steric interactions.

All calculations were performed using the Cambridge Serial Total Energy Package employing the PW91 general gradient approximation functionals. Plane waves up to 25 Ry were used, similar to that in previously published calculations [8]. K-point sampling meshes equivalent to $8 \times 8 \times 1$ for a 1×1 cell were used according to Monkhorst-Pack's scheme [9]. Ultrasoft pseudopotentials were employed for all atoms in the cell [10]. Geometry optimization was performed until the residual forces on atoms were less than 0.02 eV/Å. All cells used contained 6 Si layers with the bottom two layers fixed at bulk position and terminated with H. Cell sizes were fixed to yield a calculated lattice constant of 5.423 Å, and the energies reported here are accurate to better than ± 5 meV [11].

The total energy of a fully halogenated Si(100)-2×1 surface was calculated. Then, by selectively replacing halogen-filled dimers (i.e., dimers containing two halogen atoms) with hydrogen-filled dimers, halogen repulsions in the dimer row or dimer bond directions (referred to as α and β interactions, respectively) were removed. Since the Si-H bond is very short (~ 1.5 Å), and H and Si have similar electronegativities [12], interactions between hydrogen and halogen atoms can be reasonably neglected. A series of 4×4 cells was studied (see Fig. 3). The first two represent a fully halogenated and hydrogenated surface, while the last describes two half hydrogen–half halogen surface patterns designed to capture these α and β interactions. The α and β were then calculated as $E = \frac{1}{2}[\frac{1}{2}(E_{\text{halogen}} + E_{\text{hydrogen}}) - E_{\text{halogen-hydrogen}}]$. However,

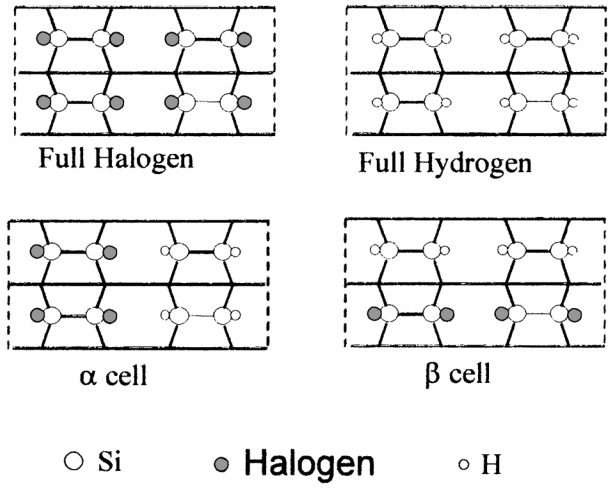

FIG. 3. The cells used in determining α and β steric repulsions. All cells are 4×4 in size and composed of four dimers.

the contribution from second-nearest-neighbor interactions (γ) is unaccounted for (see Fig. 3). To estimate this interaction, we considered an additional 4×4 cell, composed of two diagonally positioned halogen-filled dimers. We found that γ is $\sim$5 meVwith only minor variations for different halogens due to offsetting electrostatic and steric interactions [4]. For the purposes of the present study, γ interactions are negligibly small and do not contribute significantly to roughening (see below).

Table I lists the calculated values of α and β for each halogen. α is about twice β since α involves interactions between two pairs of halogens, whereas β involves just a single pair (see Fig. 4). The calculations also reveal that the dimer and silicon-halogen bond lengths were essentially unaffected ($\Delta d < 0.01$ Å) by the presence of neighboring hydrogen-filled dimers. However, the silicon-halogen bond angle is relaxed (in the case of Br) from 108.6° (full Br cell) to 111° (Br α cell), in agreement with the STM results in Fig. 2 [13]. Bond angle relaxation of this kind was previously reported by de Wijs and Selloni for the case of a periodic Br-passivated Si(100)-3×2 surface [8].

To calculate the roughening energy, we start with a perfect, fully halogenated 2×1 surface and introduce a primary roughening event that creates an infinitely long DV string and single dimer row island, which we assume do not intersect. Then, in a secondary roughening event, the DV string is dissociated into two SV strings separated by single or multiple (n) dimer rows, creating a local 3×2 or $[(2n + 1) \times 2]$ structure [5,8]. The contributions of the DV string and single dimer row island to the surface energy are identical, and each is equivalent to the formation energy for two S_A steps. The Si(100) S_A step energy is estimated to be 50 meV$/2a$ ($a = 3.84$ Å) [14]. Thus, primary roughening requires the formation of four S_A steps, whereas secondary roughening requires two additional S_A steps (see Fig. 4). The validity of this approach is demonstrated by the recent work of de Wijs and Selloni where the roughening energy of the periodic 3×2 structure was calculated as 96 meV$/2a$, i.e., twice the S_A step energy [8].

The total energy is the sum of the surface energy increase together with the changes in the steric interactions relative to that on the perfect surface. Using Fig. 4, straightforward counting shows that the total energy increase (per unit step length) due to primary roughening is $4S_A - 2\alpha - 4\beta - 16(\gamma - \gamma')$, whereas secondary roughening costs an additional $2S_A - \alpha - 2\beta - 8(\gamma - \gamma')$. Here γ' is the second-nearest-neighbor interaction between adjacent terraces (see Fig. 4). Since γ and γ' are small and exactly offset each other, second-nearest-neighbor interactions contribute little to roughening. The results for Br, Cl, and F surfaces are shown in Table I. With the exception of F, roughening is always energetically favored, and the driving force is greatest for larger halogens. While steric effects are primarily responsible for roughening, electrostatic dipole repulsions also play a role, and in the case of F, are the dominant contributions to the repulsion energy.

Since roughening is always entropically favored, for Br and Cl it is spontaneous at all temperatures, and will be pronounced whenever there is sufficient thermal energy to overcome the activation energies involved. In agreement with experiment, roughening is most pronounced for Br, which exhibits both primary and secondary roughening, the latter especially at higher temperature. Roughening is also observed for Cl but the temperatures are significantly higher [4]. In the case of F, sterically driven roughening is not favored. However, F surfaces are intrinsically rough [15,16], and in industry roughening is controlled

TABLE I. Steric and roughening energies (per 7.68 Å): The first two columns list α and β steric energies for Br, Cl, and F. The last two columns compare the energies for primary and secondary roughening assuming $S_A = 50$ meV$/2a$.

	Intra-row α (meV)	Inter-row β (meV)	Primary[a] $4S_A - 2\alpha - 4\beta$ (meV)	Secondary[a] $2S_A - \alpha - 2\beta$ (meV)
Bromine	106	52	−220	−110
Chlorine	61	26	−26	−13
Fluorine	24	14	96	48

[a]Neglects γ and γ' contributions.

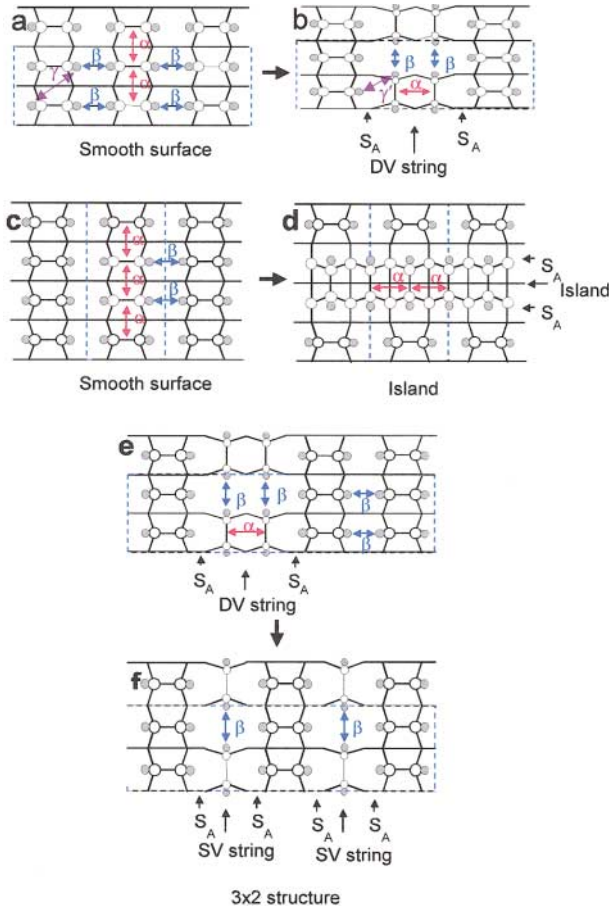

FIG. 4 (color). The change in steric interactions due to primary and secondary roughening. (a)–(f) The changes in the nearest-neighbor interactions (α and β) during roughening. For clarity, only a single second-nearest-neighbor interaction (γ and γ') is shown in (a) and (b). Relative to the perfect surface, per unit step length, the creation of a DV string (a) $\rightarrow$ (b) involves a reduction of $2\alpha + 4\beta + 12\gamma$ interactions while $\alpha + 2\beta + 4\gamma + 8\gamma'$ interactions are introduced. During island creation (c) $\rightarrow$ (d), $3\alpha + 2\beta + 12\gamma$ are removed and $2\alpha + 4\gamma + 8\gamma'$ are introduced. The sum $(2\alpha + 4\beta + 16\gamma - 16\gamma')$ is the total reduction in repulsive interactions during primary roughening. In the case of secondary roughening (e) $\rightarrow$ (f), halogen repulsions are further reduced by $\alpha + 2\beta + 8\gamma - 8\gamma'$. For both roughening processes, the second-nearest-neighbor interactions (γ and γ') effectively cancel out and are neglected (see text).

either by using Cl or by incorporating F into less reactive molecules (e.g., CF_4), thereby moderating its reactivity [17]. The present study demonstrates that Cl surfaces spontaneously roughen and suggests that modified F surfaces may also roughen, the latter being due to steric interactions introduced by adsorbed CF_x species. However, atomically smooth etch morphologies may be attainable provided sterically confined etchants can be developed or etching can be accomplished at low temperatures where roughening is inaccessible.

The roughening phenomenon described here has important implications for the mechanism of chemical etching itself. Terrace roughening facilitates etching by generating step and kink sites that are susceptible to chemical attack. The etch rate and the degree of continuous roughening are both controlled by the temperature and the halogen coverage. However, in contrast to what is currently held, the presence of primary and secondary roughening is not necessarily indicative of etching [1]. Instead, roughening is an inherent property of halogen-terminated surfaces and must be directly accounted for in all models of Si(100) etching and processing.

The authors thank the NSF and Science Foundation Ireland for funding.

Note added.—After submission of this work, a paper [18] was published that discusses roughening in this same system. The mechanism cited by the authors requires the presence of vacant sites and is fundamentally different from the sterically induced roughening phenomenon identified here.

*To whom correspondence should be addressed.
Present address: Department of Chemistry, Trinity College, Dublin, Ireland.

[1] J. H. Weaver and C. M. Aldao, in *Morphological Organization in Epitaxial Growth and Removal*, edited by M. G. Lagally and Z. Zhang, World Scientific Series on Directions of Condensed Matter Physics Vol. 14 (World Scientific, Singapore, 1998), and references therein; G. A. de Wijs and A. Selloni, Phys. Rev. Lett. **78**, 4877 (1997).
[2] R. D. Schnell, D. Rieger, A. Bogen, K. Wandelt, and W. Stienmann, Solid State Commun. **53**, 205 (1985).
[3] J. J. Boland, Adv. Phys. **42**, 129 (1993).
[4] D. Chen and J. J. Boland (to be published).
[5] M. Chander, Y. Z. Li, D. Rioux, and J. H. Weaver, Phys. Rev. Lett. **71**, 4154 (1993).
[6] C. F. Herrmann and J. J. Boland, Phys. Rev. Lett. **87**, 115503 (2001).
[7] C. F. Herrmann and J. J. Boland, J. Phys. Chem. B **103**, 4207 (1999).
[8] G. A. de Wijs and A. Selloni, Phys. Rev. B **64**, 041402 (2001).
[9] H. J. Monkhorst and J. P. Pack, Phys. Rev. B **13**, 5188 (1976).
[10] D. Vanderbilt, Phys. Rev. B **41**, 7892 (1990).
[11] A. Ramstad, G. Brocks, and P. J. Kelly, Phys. Rev. B **51**, 14 504 (1995).
[12] A. L. Allred, J. Inorg. Nucl. Chem. **17**, 215 (1961).
[13] The calculated bond tilt cannot fully explain the observed contrast in the STM image. There is a significant electronic contribution which will be described elsewhere.
[14] H. J. Zandvliet, Rev. Mod. Phys. **72**, 593 (2000).
[15] C. W. Lo *et al.*, Surf. Sci. **292**, 171 (1993).
[16] C. J. Wu and E. A. Carter, J. Am. Chem. Soc. **113**, 9061 (1991).
[17] S. Wolf and R. N. Tauber, *Silicon Processing for the VLSI Era* (Lattice, Sunset Beach, 2000).
[18] K. S. Nakayama, E. Graugnard, and J. H. Weaver, Phys. Rev. Lett. **88**, 125508 (2002).